

Differential Response to Abiraterone Acetate and Di-*n*-butyl Phthalate in an Androgen-Sensitive Human Fetal Testis Xenograft Bioassay

Daniel J. Spade, Susan J. Hall, Camelia M. Saffarini, Susan M. Huse, Elizabeth V. McDonnell, and Kim Boekelheide¹

Department of Pathology and Laboratory Medicine, Brown University, Providence, RI, USA

¹To whom correspondence should be addressed at Department of Pathology and Laboratory Medicine, Brown University, Box G-E5, 70 Ship Street, Providence, RI 02912. Fax: (401) 863-9008. E-mail: kim_boekelheide@brown.edu.

Received September 11, 2013; accepted November 14, 2013

In utero exposure to antiandrogenic xenobiotics such as di-*n*-butyl phthalate (DBP) has been linked to congenital defects of the male reproductive tract, including cryptorchidism and hypospadias, as well as later life effects such as testicular cancer and decreased sperm counts. Experimental evidence indicates that DBP has *in utero* antiandrogenic effects in the rat. However, it is unclear whether DBP has similar effects on androgen biosynthesis in human fetal testis. To address this issue, we developed a xenograft bioassay with multiple androgen-sensitive physiological endpoints, similar to the rodent Hershberger assay. Adult male athymic nude mice were castrated, and human fetal testis was xenografted into the renal subcapsular space. Hosts were treated with human chorionic gonadotropin for 4 weeks to stimulate testosterone production. During weeks 3 and 4, hosts were exposed to DBP or abiraterone acetate, a CYP17A1 inhibitor. Although abiraterone acetate (14 d, 75 mg/kg/d po) dramatically reduced testosterone and the weights of androgen-sensitive host organs, DBP (14 d, 500 mg/kg/d po) had no effect on androgenic endpoints. DBP did produce a near-significant trend toward increased multinucleated germ cells in the xenografts. Gene expression analysis showed that abiraterone decreased expression of genes related to transcription and cell differentiation while increasing expression of genes involved in epigenetic control of gene expression. DBP induced expression of oxidative stress response genes and altered expression of actin cytoskeleton genes.

Key Words: xenograft; Hershberger assay; antiandrogen; abiraterone acetate; di-*n*-butyl phthalate; CYP17A1.

In the rat, disruption of fetal androgen signaling by antiandrogenic xenobiotics can produce dramatic negative consequences for the male reproductive tract (Rider *et al.*, 2008). It has been hypothesized that antiandrogens have similar effects in the human fetal male reproductive tract. These effects are included as part of a hypothesized testicular dysgenesis syndrome (TDS), wherein perturbation of fetal Sertoli and Leydig cell function, through mechanisms including impaired fetal androgen signaling, is associated with cryptorchidism and

hypospadias, decreased adult male fertility, and increased testicular cancer risk in adulthood (Lottrup *et al.*, 2006; Toppari *et al.*, 2010). However, the impact of some putative antiandrogens, particularly phthalates, on the development of the human male reproductive tract is unclear.

Phthalates are organic esters used as plasticizers, to which humans are almost universally exposed. In the rat, phthalates interfere with male reproductive tract development to produce TDS endpoints (Howdeshell *et al.*, 2008). However, a mechanistic association between phthalate exposure and TDS outcomes has not been established, and effects of fetal phthalate exposure appear species specific. *In utero* di-*n*-butyl phthalate (DBP) exposure reduces fetal testicular testosterone in the rat but not in the mouse (Gaido *et al.*, 2007; Johnson *et al.*, 2012). Neither model is necessarily predictive of the human response.

In rodents, the effects of suspected antiandrogens can be assessed directly. *In utero* exposure studies assess testicular hormone levels and androgen-sensitive endpoints such as anogenital distance, nipple retention, hypospadias, and cryptorchidism (Howdeshell *et al.*, 2008; Rider *et al.*, 2008). The Hershberger assay allows for quantification of antiandrogenic effects in juvenile rats, with endpoints including serum hormones and the weights of androgen-responsive accessory sex organs (Gray *et al.*, 2005). However, there is no means by which to study the physiological effects of antiandrogens in intact human fetal testis. To address this issue, human fetal testis xenograft models have been developed. In 2 studies, DBP exposure induced multinucleated germ cells (MNGs) in xenografts but had no effect on expression of genes related to androgen biosynthesis (Heger *et al.*, 2012), or host serum testosterone or seminal vesicle weight (Mitchell *et al.*, 2012). No study to date has demonstrated inhibition of testosterone biosynthesis in human fetal testis xenografts.

Abiraterone acetate is an irreversible steroidal CYP17A1 inhibitor (Jarman *et al.*, 1998), which decreases testosterone in *in vivo* rodent studies (Duc *et al.*, 2003; Haidar *et al.*, 2003) and is used clinically for treatment of castration-resistant prostate

cancer (de Bono *et al.*, 2011). We hypothesized that abiraterone acetate, but not DBP, would inhibit testosterone biosynthesis in human fetal testis xenografts. The model previously published by Heger *et al.* (2012) was modified to optimize measurements of antiandrogenic effects, using a human chorionic gonadotropin (hCG)–stimulated castrated mouse host, similar to Mitchell *et al.* (2012). This xenograft bioassay allowed for the measurement of host serum hormones and androgen-sensitive accessory sex organ weights, parallel to the Hershberger bioassay in the rat, to quantify inhibition of androgen signaling in human fetal testis.

MATERIALS AND METHODS

Animal care. Adult male athymic nude mice (CrI:NU(NCr)-*Foxn1*tm, strain code 490) were obtained from Charles River Laboratories (Wilmington, Massachusetts) and housed in the Brown University Animal Care Facility under a 12:12 h light-dark cycle with controlled temperature and humidity. Mice were given free access to water and Purina Rodent Chow 5001 (Farmer's Exchange, Framingham, Massachusetts). All animal care protocols were approved by the Brown University Institutional Animal Care and Use Committee.

Donor information. Human fetal testis samples originated from spontaneous pregnancy losses and were donated with full informed consent, as previously described (De Paepe *et al.*, 2012), in accordance with protocols approved by the Women and Infants Hospital of Rhode Island Institutional Review Board. At the time of donation, the gestational age of the fetus was recorded, as well as any relevant notes regarding the pregnancy and the post-mortem interval from delivery until the time of xenograft surgery (Table 1). Human fetal testis tissue was transported from Women and Infants Hospital, Providence, RI, to Brown University on ice in Leibovitz's L15 media supplemented with penicillin, streptomycin, and gentamicin (each 50 µg/ml). Testis tissue was dissected under aseptic conditions. A small piece of each testis was fixed immediately in 10% neutral-buffered formalin (NBF), another piece was snap frozen in liquid nitrogen, and the remainder was prepared for xenograft surgery. All unimplanted samples were morphologically normal, as verified by histopathology, and no sample was used after a postmortem interval greater than 36 h.

Xenograft surgery and experimental protocol. Testis tissue was dissected into 64 pieces of approximately 1 mm³ for implantation into 8 hosts, with 8 xenografts per host. Within each experiment, 8 xenografted host mice and 6 ungrafted control ("sham") mice were divided into treatment (abiraterone or DBP) or vehicle groups. The exception to this design was sample 26 (Table 1), in which 2 grafted mice were assigned to control and treated groups,

respectively, and 2 "sham" mice were treated with DBP; there was no vehicle-treated sham group. The sample size for all treatment groups, using the donor as the unit of replication, was $n = 3$, except for the sham-vehicle group in the DBP studies ($n = 2$). Xenograft surgery was performed using an abdominal incision and renal subcapsular xenograft site, as described by Heger *et al.* (2012). Immediately prior to xenografting, the host or sham mouse was castrated using an abdominal approach through the same midline incision. Both testes and epididymides were removed in their entirety. The vas deferens and associated vasculature were cauterized using a stainless steel cautery and cut, and any connective tissue was trimmed to allow removal of the testis and epididymis.

Following surgery, hosts were given 20 IU hCG sc 3 times per week for 4 weeks. During the final 2 weeks, mice were also administered daily oral gavage of 75 mg/kg/d abiraterone acetate or 500 mg/kg/d DBP (Sigma-Aldrich, St Louis, Missouri), or matching vehicle control (diH₂O with approximately 0.3% Tween-20 or corn oil, respectively), according to the treatment designations in Table 1. Abiraterone vehicle was chosen based on similarity with Duc *et al.* (2003). Abiraterone acetate tablets (Zytiga, Centocor Ortho Biotech, Horsham, Pennsylvania), obtained by donation of Dr Mark Sigman and Dr Kathleen Huang at Rhode Island Hospital, were ground into a powder using a mortar and pestle and added to the appropriate volume of Tween-20/distilled water solution to produce a uniform suspension. Six hours after the final dose, hosts were euthanized by overdose of isoflurane. Blood was collected by cardiac puncture. Accessory sex organs and kidneys containing xenografts were removed. Xenografts designated for gene expression analysis were snap frozen in liquid nitrogen. Xenografts intended for histology and immunohistochemistry were fixed in NBF or modified Davidson's fixative (MDF). MDF was changed to NBF after 24 h, and xenografts were stored in NBF until further processing. Accessory sex organs, including the seminal vesicles, anterior prostate, and levator ani-bulbocavernosus muscles (LABC), were dissected from hosts according to the method of Gray *et al.* (2005); however, seminal vesicles and anterior prostate were dissected and weighed separately. The Hershberger assay also makes use of the ventral prostate, Cowper's gland, and glans penis. We dissected ventral, lateral, and dorsal prostate, but found the weights to be highly variable in our mice, making anterior prostate a more consistent endpoint. The mouse Cowper's gland is smaller than that of the rat and did not provide a reasonable dissection endpoint. We also decided not to use the glans penis, as it is no longer androgen sensitive in the adult hosts, unlike the juvenile rats used for the Hershberger assay. Blood was allowed to coagulate for at least 10 min at room temperature and then centrifuged for 10 min at 3000 · g to obtain serum. Serum was frozen at -80°C and shipped on dry ice to the University of Virginia Center for Research in Reproduction, where radioimmunoassays for testosterone and progesterone were performed. Reported coefficients of variation for all radioimmunoassays performed at this facility in 2012 were 4.0% intra-assay and 7.1% interassay for testosterone, and 4.3% intra-assay and 7.3% interassay for progesterone.

Histological analysis. Xenografts were dehydrated in a series of graded ethanols and embedded in Technovit 7100 glycol methacrylate (Heraeus Kulzer GmBH, Wehrheim, Germany). Three serial 5 µm sections were cut from the

TABLE 1
Donors and Experimental Conditions

Donor ID	GA (weeks)	PMI (h)	Surgery Date	Treatment	Notes
17,18	22	20	May 18, 2012	Abiraterone	Twins
19	20	16.5	September 11, 2012	DBP	PROM; no prenatal care
20	16	33	October 12, 2012	DBP	
23	20	17	November 29, 2012	Abiraterone	
25	20	21	January 9, 2013	Abiraterone	
26	20	12	March 1, 2013	DBP	No vehicle-treated sham

Treatments: abiraterone—14 d 75 mg/kg/d abiraterone acetate or vehicle (distilled water with Tween-20) po. DBP—14 d 500 mg/kg/d DBP or vehicle (corn oil) po. Both treatments followed 14 d 20 IU hCG sc 3 times per week; hCG treatment continued concurrently with DBP or abiraterone treatment.

Abbreviations: DBP, di-*n*-butyl phthalate; GA, gestational age; PMI, postmortem interval; PROM, premature rupture of membranes.

approximate center of the graft. Total germ cells and MNGs were counted on the second section using an Olympus BH-2 microscope (Olympus, Center Valley, Pennsylvania), as described in Heger *et al.* (2012), using the first and third sections for confirmation when possible. The second section was scanned into an Aperio ScanScope CS (Aperio Technologies, Vista, CA) at $\times 40$ magnification to quantify seminiferous cord area and total xenograft cross-sectional area in square millimeters. These measures were used to calculate the ratio of germ cells to seminiferous cord cross-sectional area and the percentage of germ cells that were multinucleated.

Immunohistochemistry. Additional xenografts were processed and embedded in paraffin, trimmed to their approximate center, and sectioned at 5 μm . Sections were deparaffinized in xylene and rehydrated in graded ethanols. Antigen retrieval was performed in citrate buffer, pH 6.0, for 20 min in a vegetable steamer, and then was allowed to cool on the bench top for 20 min. Endogenous peroxidase was blocked for 30 min in a 3% solution of hydrogen peroxide in methanol. Avidin/biotin blocking was performed using the Vector Avidin/Biotin Blocking Kit (Vector Laboratories, Burlingame, California). Blocking and antibody binding were performed using the Vector Laboratories Mouse on Mouse (M.O.M.) Basic Kit. Tissue sections were incubated with mouse monoclonal Cytochrome P450 17A1 (CYP17A1) antibody, clone 3F11 (Novus Biologicals, Littleton, Colorado) at a 1 $\mu\text{g}/\text{ml}$ dilution, and a secondary antibody was applied according to the manufacturer's instructions. Avidin/biotin-based peroxidase conjugation was performed using the Vectastain ABC Elite kit (Vector Laboratories), and staining was developed using Vector Laboratories DAB (3,3'-diaminobenzidine) Peroxidase Substrate Kit.

Gene expression analysis. Snap-frozen xenografts were pooled by donor and treatment group to provide sufficient tissue for RNA extraction and to allow the donor to be treated as the unit of replication for real-time PCR analysis. RNA was extracted from snap-frozen xenograft tissue using the AllPrep DNA/RNA Mini Kit (Qiagen, Valencia, California) and on-column DNase treatment with the Qiagen RNase-free DNase Set, according to the manufacturer's instructions. DNA was retained for a separate study. RNA was further purified by overnight precipitation at -80°C with 0.1 volume of 3M sodium acetate, pH 5.2, and 3 volumes of ethanol. Precipitated RNA was centrifuged for 30 min at 16 100 $\cdot\text{g}$ in an Eppendorf 5414 D microcentrifuge at 4°C , washed with ice-cold 75% ethanol, and reconstituted in nuclease-free water. RNA concentration and purity were assessed using the Nanodrop ND-1000 spectrophotometer (Thermo Fisher Scientific, Waltham, Massachusetts) (average A_{260}/A_{280} : 1.75, range = 1.6–1.93; average A_{260}/A_{230} : 2.18, range = 1.73–2.42). RNA integrity was assessed using the Agilent 2100 Bioanalyzer (Agilent Technologies, Santa Clara, California) (average RNA Integrity Number: 7.92, range = 5.3–9.6). Gene expression analysis was performed using both Affymetrix Human Gene 1.0 ST microarrays (Affymetrix, Santa Clara, California) and RT² Profiler PCR Arrays (SA Biosciences, Valencia, California), according to manufacturer's instructions.

To determine the reliability of the microarray-based gene expression analysis, we developed a custom gene expression RT² PCR Profiler Array (SA Biosciences). The array primarily consisted of genes involved in steroid hormone biosynthesis, including *STAR*, *CYP11A1*, *CYP17A1*, *HSD17B1*, *HSD17B2*, *HSD17B3*, *SRD5A1*, *SRD5A2*, *HSD3B1*, *HSD3B2*, *CYP19A1*, *CYP11B1*, *CYP11B2*, *CYP21A2*, *HSD11B1*, *HSD11B2*, *AKR1C1*, *AKR1C3*, *POR*, *FDX1*, *FDXR*, *CYB5A*, *H6PD*, and *HSD17B6*, the roles of which are reviewed by Miller and Auchus (2011). The hormone receptors *AR*, *LHCGR*, *FSHR*, *ESR1*, *ESR2*, and *PGR* were also included. Despite their primary expression in hypothalamus and pituitary, *GNRH1*, *GNRH2*, and *GNRHR* were included because they are reportedly expressed in fetal rat gonads (Botte *et al.*, 1998). Also included were 2 genes, *INSL3* and *SCARB1*, which are known to respond to DBP in short-term rodent studies (Heger *et al.*, 2012); 3 inhibin genes, *INHA*, *INHBA*, and *INHBB*, because serum inhibin B is altered by some testicular toxicants (Moffit *et al.*, 2013); and 2 genes, *KIT* and *KITLG*, related to Sertoli-germ cell contact (Unni *et al.*, 2009).

To determine the best combination of the 5 housekeeping genes (HKGs) to use for analysis of the PCR panel, real-time PCR array data were first analyzed using NormFinder (Andersen *et al.*, 2004) and BestKeeper (Pfaffl *et al.*, 2004). These 2 algorithms determined *RPLP1* and *HPRT1* to be the most stable HKGs, respectively, and found *HSP90AB1* and *GAPDH* to be the least stable.

GAPDH had particularly poor correlation ($r = 0.77$) with the other HKGs, according to BestKeeper and so was removed from the HKG set. The remaining 4 HKGs each had a correlation of $r \geq 0.91$ with each other and were deemed an appropriate set for normalization. PCR array results were calculated using the $\Delta\Delta C_T$ method (Livak and Schmittgen, 2001), with the arithmetic mean C_T of *HPRT1*, *RPLP1*, *B2M*, and *HSP90AB1* acting as the HKG value.

Data analysis and statistics. For serum hormone, histology, immunohistochemistry, and organ weight data, within-experiment replicates were averaged by treatment group so that the donor (tissue sample) was treated as the unit of replication, giving a sample size of $n = 3$, except for the vehicle-treated sham group in the DBP experiments, where $n = 2$. Treatment effects within sham groups were not significant for any comparison using 1-tailed *t* test or paired *t* test, so the mean of all values was used as a reference. The effect of treatment on implanted hosts or xenograft tissue was analyzed by a 1-tailed paired *t* test ($n = 3$). In the case that data failed the normality assumption by Shapiro-Wilk test, they were analyzed using a Wilcoxon signed-rank test. Microarray data were processed in the R software environment (R Core Team, 2012), using the RMA algorithm (R package oligo) (Carvalho and Irizarry, 2010) for probe-level summarization and preprocessing with ComBat (Leek *et al.*, 2012) for batch correction. Gene annotation information was joined to the expression data using the hugene10sttranscript-cluster.db package (Li, 2013). Three paired analyses were performed using the limma package in R (commands *lmfit* and *eBayes*), with the Benjamini-Hochberg correction for multiple comparisons (Smyth, 2005): vehicle-treated xenografts versus unimplanted testis ($n = 5$), abiraterone-treated xenografts versus matched control xenografts ($n = 3$), and DBP-treated xenografts versus matched control xenografts ($n = 3$). For the vehicle versus unimplanted comparison, statistical significance was considered as $q < 0.05$ with a fold change greater than 2.0. For the latter 2 comparisons, there were no *q*-significant genes, so genes with $p < .05$ and fold change > 1.5 are listed. Raw and normalized microarray data were submitted to the NCBI Gene Expression Omnibus database (series no. GSE49244), in accordance with MIAME standards (Brazma *et al.*, 2001). Principal component analysis (PCA) was performed on median-centered microarray data using the PCA module within GenePattern (Reich *et al.*, 2006). Following gene-level analysis, functional enrichment analysis was performed using Gene Set Enrichment Analysis (Subramanian *et al.*, 2005) to identify Gene Ontology (GO) classes of genes that were enriched in the microarray data, performing 1000 permutations using the default settings. Real-time PCR data were analyzed using paired *t* tests to compare vehicle with unimplanted samples ($n = 5$), as well as DBP and abiraterone with respective vehicle samples ($n = 3$).

RESULTS

Xenograft Morphology

Germ cells were visible in xenografts from all treatment groups (Figs. 1A–C). Leydig cells from all xenografts expressed CYP17A1 highly, and in the cytoplasm only (Figs. 1D–F), indicating potential for testosterone biosynthesis in all treatment groups. Neither abiraterone (Figs. 1G and H) nor DBP (Figs. 1I and J) treatment resulted in significant differences in the proportion of germ cells that were multinucleated (Figs. 1A and C) or in the number of germ cells per unit of seminiferous cord cross-sectional area (Figs. 1B and D). However, DBP-treated xenografts exhibited a trend toward higher MNG numbers compared with vehicle-treated xenografts (Fig. 1C, $p = .051$, 1-tailed paired *t* test).

Host Serum Hormone Status

Serum hormone levels were consistently lower in sham than in implanted mice and did not differ by treatment. Abiraterone treatment reduced host serum testosterone levels to approximately 20% of the concentration in vehicle-treated host serum

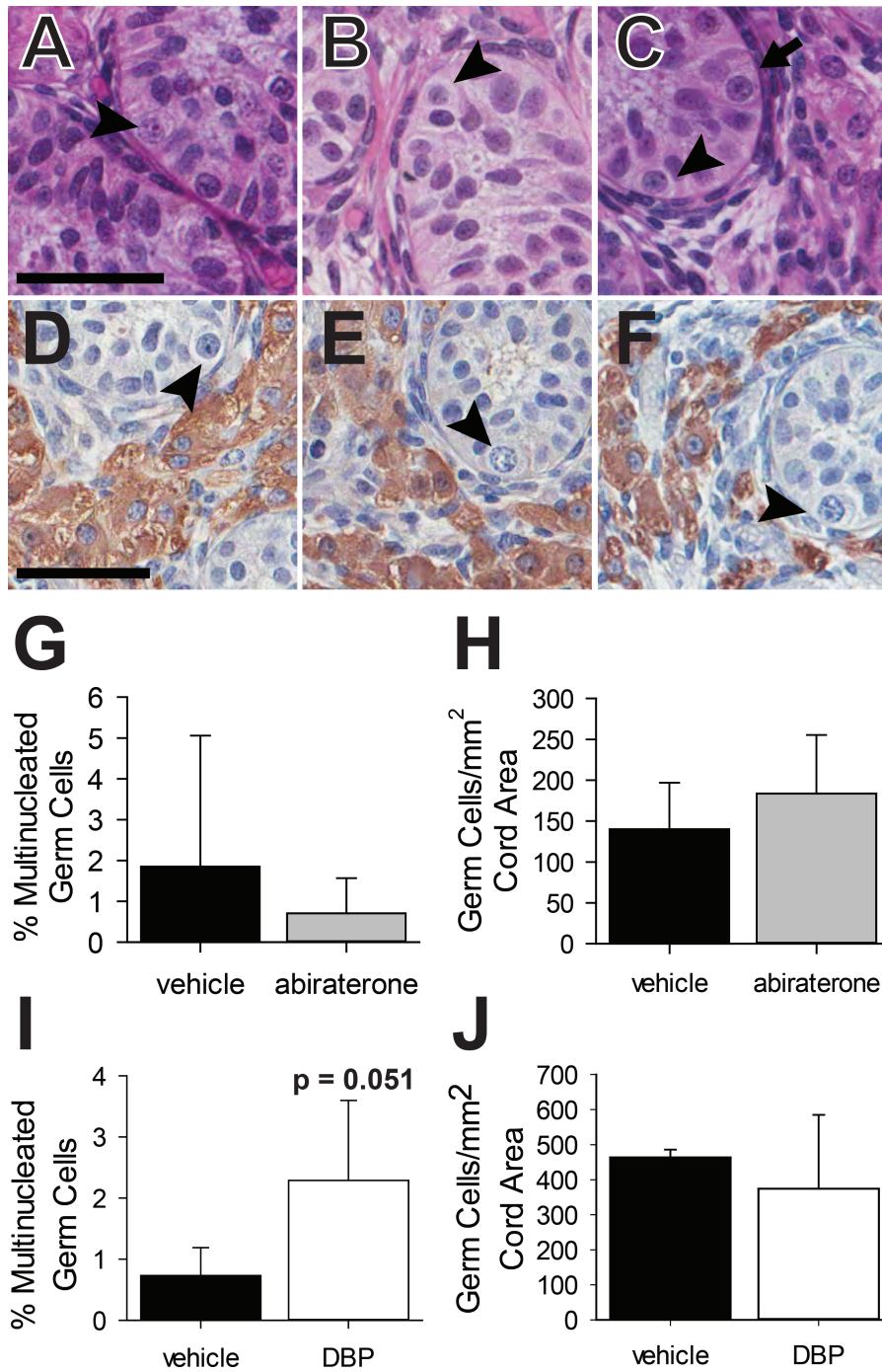


FIG. 1. Xenograft morphology. Xenografts treated with vehicle (A), 75 mg/kg/d abiraterone acetate (B), and 500 mg/kg/d di-*n*-butyl phthalate (DBP) (C) showed normal fetal testis morphology. Germ cells (arrowheads) were present in all treatment groups (A–C: hematoxylin and eosin; scale bar = 50 μ m). Arrow in (C) labels a multinucleated germ cell (MNG) in a DBP-treated xenograft. CYP17A1 was expressed only in the cytoplasm of Leydig cells (D–F; hematoxylin counterstain; scale bar = 50 μ m). No difference in staining intensity or localization was evident among xenografts treated with vehicle (D), abiraterone acetate (E), and DBP (F). Frequency of MNGs, expressed as a percentage of total germ cells, was not significantly different following abiraterone acetate (G) or DBP (I) treatment ($n = 3$, 1-tailed paired t test), but DBP treatment resulted in a trend toward increased MNGs ($p = .051$). The number of germ cells per unit seminiferous cord area did not differ significantly following either treatment (H, J, $n = 3$, 1-tailed paired t test). The full color image is available online.

at the time of euthanasia (Fig. 2A, $p < .01$). The resulting serum testosterone concentration was similar to the ungrafted sham hosts (reference line in 2A). Serum progesterone concentration

trended toward an increase in host serum, concomitant with decreasing testosterone, but this was not statistically significant (Fig. 2B). This does suggest, however, that abiraterone is acting

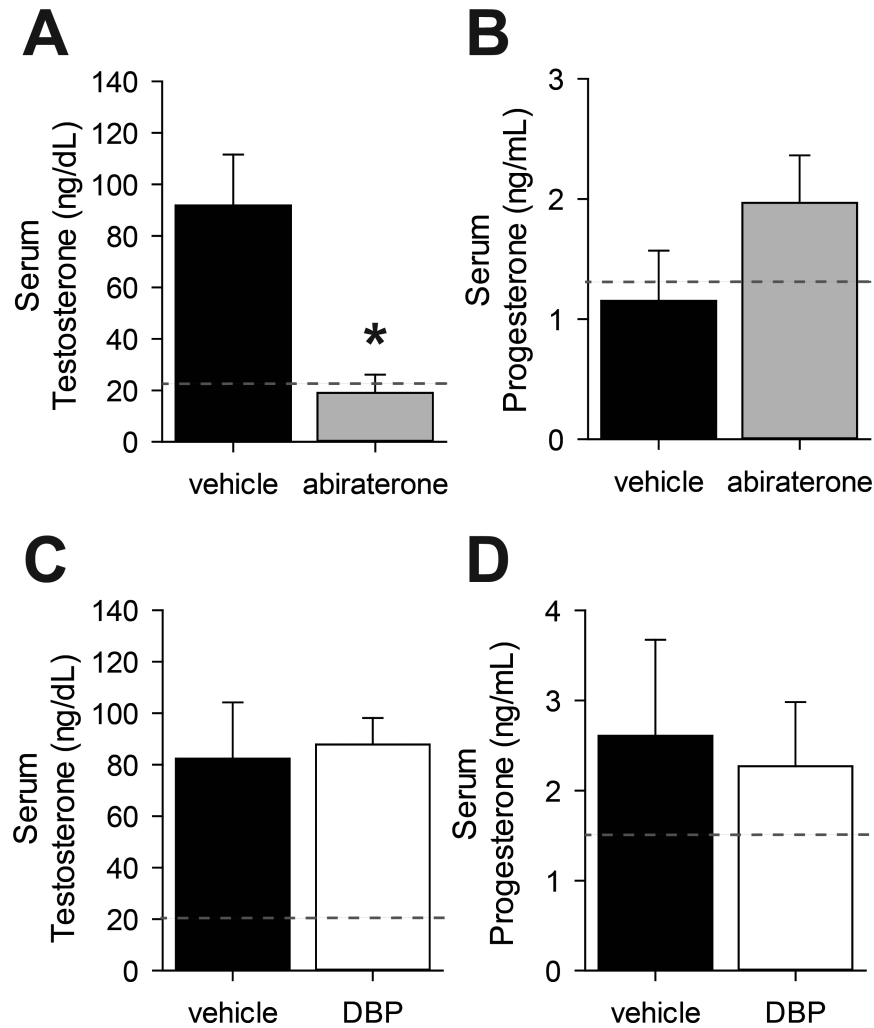


FIG. 2. Host serum hormones. Hosts receiving 75 mg/kg/d abiraterone acetate had significantly lower serum testosterone (A) and trended toward higher serum progesterone (B) than vehicle-treated hosts. Serum testosterone (C) and progesterone (D) did not differ significantly between 500 mg/kg/d di-*n*-butyl phthalate (DBP) and vehicle-treated hosts. Dotted reference line indicates average value for sham mice. * $p < .05$, 1-tailed paired t test, $n = 3$.

in human fetal Leydig cells through inhibition of CYP17A1, as serum progesterone increases with CYP17A1 inhibition (Laier *et al.*, 2006). Conversely, DBP treatment did not reduce host serum testosterone or increase host serum progesterone (Figs. 2C and D).

The weights of accessory sex organs—seminal vesicles, anterior prostate, and LABC—were also consistently lower in sham than in implanted hosts and did not differ by treatment. Seminal vesicle and LABC weights were significantly reduced ($p < .05$) in abiraterone-treated hosts compared with vehicle-treated hosts (Figs. 3B–D). DBP treatment resulted in no significant reduction in host accessory sex organ weights (Figs. 3F–H). The weights of all 3 accessory sex organs were significantly correlated (Spearman's ρ) with serum testosterone at the time of euthanasia (Figs. 3J–L). However, ρ values for the 3 comparisons ranged from 0.638 to 0.696, indicating a moderate strength of correlation. Accessory sex organ

weights are likely to be more representative of treatment-derived antiandrogenic effects over the course of the entire 14-d exposure period compared with the more stochastic measurement of serum testosterone. Neither treatment had a significant effect on host body weight (Figs. 3A and E), confirming that neither treatment caused gross toxicity. Of 78 total host and sham mice, there was one fatality, which occurred prior to treatment. Body weight, unlike accessory sex organ weights, was not significantly correlated with host serum testosterone (Fig. 3I).

Microarray Analysis

The results of PCA indicated that unimplanted samples had relatively similar overall gene expression profiles, whereas all of the implanted xenografts formed a diffuse cluster with no treatment-driven separation. The first 3 principal components described 54.48% of variation in the data set (Fig. 4A).

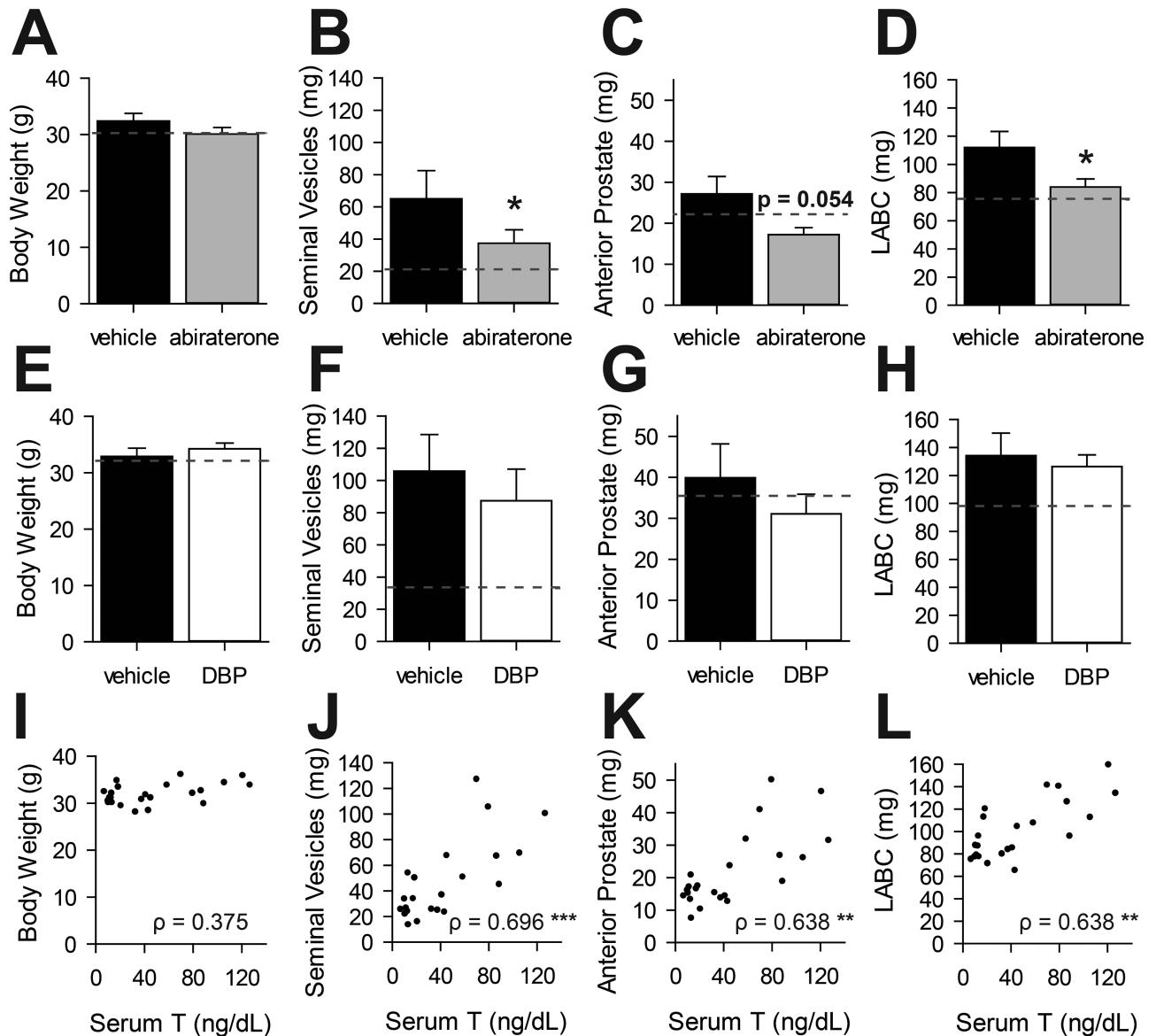


FIG. 3. Host accessory sex organ weights. Body weight of host mice was unaffected by treatment with either abiraterone acetate or DBP (A, E). Abiraterone acetate (75 mg/kg/d) significantly reduced seminal vesicle weight (B) and levator ani-bulbocavernosus muscle (LABC) weight (D), but not anterior prostate weight (C). Di-*n*-butyl phthalate (DBP, 500 mg/kg/d) did not significantly reduce the weights of any of the 3 accessory sex organs (F–H). One-tailed paired *t* test, *n* = 3, for all except body weights of abiraterone experiment hosts (panel A, Wilcoxon signed-rank test, *n* = 3). Seminal vesicle (J), anterior prostate (K), and LABC (L) weights were all significantly positively correlated with serum testosterone, whereas body weight (I) was not significantly correlated with testosterone (Spearman's ρ). *** p < .001, ** p < .01, * p < .05.

Gene-level microarray analysis identified 224 gene transcript clusters differentially regulated between vehicle-treated xenografts and unimplanted samples (Fig. 4B, Supplementary Table S1). Several genes with known expression and/or function in testis were also included in the list of significantly downregulated genes. These included *CT45A5*, a member of the cancer/testis antigen 45 family; the spermatogonial marker *GFRA1* and family member *GFRA3*, receptors for glial cell-derived neurotrophic factor, which functions in germ-Sertoli cell interaction; and the tudor domain-containing protein gene *TDRD1*. The most frequently

represented group of upregulated RNAs were 22 microRNAs, which suggests a strong impact of xenografting on noncoding regulatory RNAs (Supplementary Table S1). Although there were no widespread impacts on steroidogenic genes, *CYP19A1* and *STARD13* were upregulated. Beyond changes in the expression of individual genes, enrichment analysis revealed a number of GO processes and functions that were affected by both xenografting and treatment (Table 2). Xenografts showed enrichment for the mono-oxygenase activity GO term, which includes CYPs involved in steroid biosynthesis, such as *CYP19A1*, *CYP11B1*,

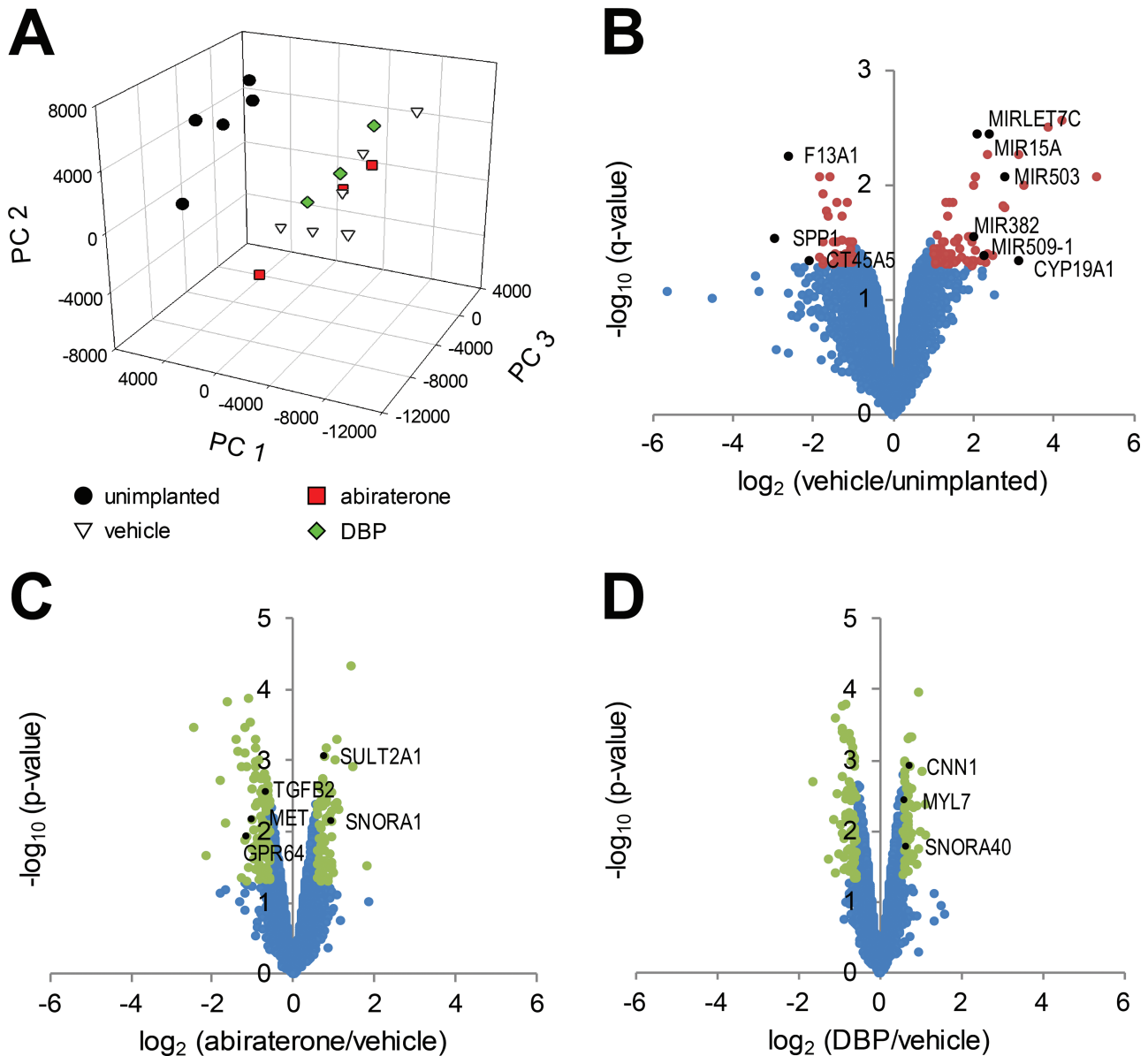


FIG. 4. Whole-transcriptome gene expression analysis. A, Principal component analysis indicated that unimplanted samples formed a cluster distinct from the xenografts, but xenografts did not resolve by treatment. A total of 55.48% of variation in microarray data was explained in the first 3 principal components (PCs). B, Microarray analysis identified 224 transcript clusters differentially regulated between vehicle-treated xenografts and the matching unimplanted samples ($q < 0.05$, expression ratio > 2 , red circles). A total of 184 transcript clusters were differentially regulated between vehicle- and abiraterone-treated xenografts (C), and 134 between vehicle- and di-*n*-butyl phthalate (DBP)-treated xenografts (D) ($p < .05$, fold change > 1.5 , green circles). None of the differences in the DBP or abiraterone treatments was significant after post hoc adjustment. Selected genes labeled in (B), (C), and (D) are discussed in the text. The full color image is available online.

and CYP11B2. Not surprisingly, steroid biosynthetic process, hormone metabolic process, and steroid binding also had strong enrichment scores, but they were not statistically significant. Ultimately, xenografts and pregrafting samples differed in expression of genes related to tissue structure, gene expression, and metabolic function. This may reflect the age of the samples, hCG stimulation, or aspects of the xenograft environment.

In contrast with the vehicle versus unimplanted comparison, the abiraterone versus vehicle-treated xenograft comparison

produced no significant genes after post hoc adjustment for multiple comparisons. At a minimum 1.5 fold change, there were 184 transcript clusters with nominal $p < .05$ (Fig. 4C, Supplementary Table S2). Changes related to endocrine processes included upregulation of *SULT2A1*, a sulfotransferase that acts on dehydroepiandrosterone, 17α -hydroxypregnenolone, and pregnenolone (Rainey and Nakamura, 2008). *TGFB2*, *MET*, and *GPR64* were downregulated after abiraterone treatment, indicating a potential negative effect of treatment on tissue

TABLE 2
Significant Gene Sets in Microarray Analysis

GO Term	GO ID	Size	ES	NES	NOM <i>p</i> value
Enriched in unimplanted versus vehicle					
Establishment of organelle localization	GO:0051656	16	0.71	1.54	.025
Transcription coactivator activity	GO:0003713	116	0.37	1.48	.025
Transcription activator activity	GO:0016563	163	0.35	1.46	.031
Regulation of transcription from RNA polymerase II promoter	GO:0006357	274	0.30	1.41	.001
Positive regulation of transcription from RNA polymerase II promoter	GO:0045944	60	0.31	1.38	.016
Enriched in vehicle versus unimplanted					
Detection of stimulus involved in sensory perception	GO:0050906	21	-0.68	-1.40	.018
Secondary active transmembrane transporter activity	GO:0015291	46	-0.51	-1.36	.008
Mono-oxygenase activity	GO:0004497	26	-0.69	-1.35	.021
Enriched in abiraterone versus vehicle					
Activation of protein kinase activity	GO:0015291	24	0.42	1.68	<.001
Basal lamina	GO:0005605	20	0.44	1.59	<.001
Maintenance of localization	GO:0051235	21	0.54	1.57	<.001
Cell projection biogenesis	GO:0030031	25	0.43	1.56	<.001
Protein homo-oligomerization	GO:0051260	21	0.42	1.56	<.001
Regulation of gene expression, epigenetic	GO:0040029	28	0.49	1.53	<.001
Protein oligomerization	GO:0051259	38	0.32	1.52	<.001
Cell matrix junction	GO:0030055	17	0.58	1.50	<.001
Adherens junction	GO:0005912	22	0.47	1.47	<.001
Cell substrate adherens junction	GO:0005924	15	0.59	1.47	<.001
Nuclear chromosome part	GO:0044454	29	0.48	1.46	<.001
Calcium ion binding		95	0.38	1.43	<.001
Enriched in vehicle versus abiraterone					
Positive regulation of transcription, DNA dependent	GO:0005509	110	-0.31	-1.62	<.001
Positive regulation of RNA metabolic process	GO:0051254	111	-0.30	-1.61	<.001
Positive regulation of cell differentiation	GO:0045597	24	-0.49	-1.57	<.001
Neuron development	GO:0048666	58	-0.44	-1.57	<.001
Positive regulation of transcription	GO:0045893	131	-0.29	-1.57	<.001
Cellular morphogenesis during differentiation	GO:0000904	44	-0.50	-1.57	<.001
Icosanoid metabolic process	GO:0006690	17	-0.65	-1.56	<.001
Regulation of blood pressure	GO:0008217	22	-0.76	-1.55	<.001
Positive regulation of nucleobase, nucleoside, nucleotide, and nucleic acid metabolic process	GO:0045935	139	-0.28	-1.54	<.001
Ligand-dependent nuclear receptor activity	GO:0004879	21	-0.55	-1.53	<.001
Neurite development	GO:0031175	50	-0.46	-1.53	<.001
Axon guidance	GO:0007411	21	-0.57	-1.51	<.001
Axonogenesis	GO:0007409	40	-0.50	-1.50	<.001
Proteinaceous extracellular matrix	GO:0005578	93	-0.38	-1.50	<.001
Extracellular matrix	GO:0031012	94	-0.37	-1.50	<.001
Intercellular junction	GO:0005911	60	-0.45	-1.49	<.001
Monovalent inorganic cation transmembrane transporter activity	GO:0015077	34	-0.53	-1.49	<.001
Glutamate signaling pathway	GO:0007215	17	-0.61	-1.48	<.001
Vitamin metabolic process	GO:0006766	17	-0.51	-1.46	<.001
Neuron differentiation	GO:0030182	73	-0.39	-1.46	<.001
Enriched in DBP versus vehicle					
Myoblast differentiation	GO:0045445	15	0.62	1.72	<.001
Biogenic amine metabolic process	GO:0006576	17	0.73	1.72	<.001
Cofactor metabolic process	GO:0051186	50	0.47	1.70	<.001
Protein N-terminus binding	GO:0047485	32	0.52	1.69	<.001
Cytoskeletal protein binding	GO:0008092	145	0.36	1.68	<.001
Amino acid derivative metabolic process	GO:0006575	24	0.62	1.68	<.001
Sphingolipid metabolic process	GO:0006665	24	0.55	1.68	<.001
Muscle cell differentiation	GO:0042692	20	0.56	1.60	<.001
Deoxyribonuclease activity	GO:0004536	18	0.51	1.59	<.001
Unfolded protein binding	GO:0051082	39	0.44	1.58	<.001
Translation initiation factor activity	GO:0003743	23	0.48	1.55	<.001
Actin binding	GO:0003779	68	0.40	1.55	<.001
Response to oxidative stress	GO:0006979	44	0.42	1.54	<.001
Actin filament	GO:0005884	16	0.58	1.54	<.001
Actin filament organization	GO:0007015	24	0.42	1.52	<.001
Mitochondrial lumen	GO:0005759	40	0.51	1.51	<.001

TABLE 2—Continued

GO Term	GO ID	Size	ES	NES	NOM <i>p</i> value
Mitochondrial matrix	GO:0005759	40	0.51	1.51	<.001
Enriched in Vehicle versus DBP					
Pattern specification process	GO:0007389	29	-0.57	-1.59	<.001
Female gamete generation	GO:0007292	16	-0.63	-1.54	<.001
Organelle localization	GO:0051640	21	-0.43	-1.51	<.001
Positive regulation of cellular component organization and biogenesis	GO:0051130	35	-0.35	-1.47	<.001
Transmembrane receptor protein tyrosine kinase signaling pathway	GO:0007169	81	-0.38	-1.38	<.001
Embryonic development	GO:0009790	53	-0.42	-1.35	<.001
Enzyme-linked receptor protein signaling pathway	GO:0007167	136	-0.34	-1.34	<.001
Cell projection	GO:0042995	98	-0.24	-1.31	<.001
Voltage-gated calcium channel activity	GO:0005245	18	-0.48	-1.27	<.001

Treatments: abiraterone—14 d 75 mg/kg/d abiraterone acetate or vehicle (distilled water with Tween-20) po. DBP—14 d 500 mg/kg/d DBP or vehicle (corn oil) po. Abbreviations: DBP, di-*n*-butyl phthalate; ES, enrichment score; NES, normalized enrichment score; NOM *p* value, nominal *p* value (no post hoc adjustment).

proliferation. Abiraterone most notably increased genes in the GO term epigenetic regulation of gene expression, including *DICER1*, *DNMT1*, *DNMT3A*, and *DNMT3B*, suggesting that abiraterone may affect epigenetic processes.

As with abiraterone, there were no genes with significant *q*-values after DBP treatment, relative to vehicle, but 134 transcript clusters had fold changes greater than 1.5 and *p* < .05 (Fig. 4D, Supplementary Table S3). These included 2 transcripts for structural genes that may be targets of DBP: *CNN1*, a component of the actin-myosin structure in smooth muscle, and the myosin light chain peptide *MYL7*. Functional enrichment analysis indicated that DBP-treated grafts were enriched for genes involved in oxidative stress response, particularly the glutathione metabolism genes *GSS*, *GPX3*, and *GLRX2*, and in actin filament genes including *ACTC1*, *ACTA1*, *MYO3A*, and *ACTN2*. DBP-treated xenografts had negative enrichment for genes related to organelle localization. These processes could be among those that are altered leading to morphological changes in the human fetal testis after DBP exposure, without effects on testosterone biosynthesis.

Real-time PCR Panel

PCR array analysis identified 5 significantly differentially regulated transcripts (*p* < .05, paired *t* test) between vehicle and unimplanted samples (Table 3). Two transcripts were differentially regulated between abiraterone and vehicle (*p* < .05, paired *t* test). No significant differences were detected between DBP-treated and vehicle xenografts. Gene expression levels determined by microarray and real-time PCR were highly concordant for 36 of the 40 target genes ($\rho = -0.909$ between microarray \log_2 intensity and real-time PCR C_t). The remaining 4 genes—*AKR1C3*, *CYP11B1*, *ESR2*, and *KIT*—were detected at higher levels by microarray than by PCR. PCR assays for these genes appeared less sensitive than microarrays, and in many cases no expression was detected. The fold changes of significant genes, as determined by either platform, were similar across the board, but statistical significance often differed based on the platform (Table 3). However, this confirms

the microarray results, which indicated that gene expression changes related to steroidogenesis are limited following 14-d exposure to abiraterone or DBP.

DISCUSSION

This is the first report of an antiandrogenic effect in a human fetal testis xenograft model. In previous studies, exposure of rodent hosts bearing rat fetal testis xenografts to DBP produced antiandrogenic effects, but these effects were not reproduced in hosts bearing human fetal testis xenografts (Heger *et al.*, 2012; Mitchell *et al.*, 2012). Here, our goal was to inhibit testosterone biosynthesis directly in human fetal testis xenografts using abiraterone acetate and to compare with the effects of DBP treatment. This makes for a particularly relevant comparison because both compounds exert their antiandrogenic effects by reducing testosterone, without antagonizing the androgen receptor. As we hypothesized, 500 mg/kg/d DBP had no effect on host serum testosterone or androgen-sensitive organ weights in our xenograft model; however, abiraterone acetate treatment dramatically reduced serum testosterone and significantly reduced seminal vesicle and LABC weights (Figs. 2 and 3). This supports the conclusions of Heger *et al.* (2012) and Mitchell *et al.* (2012) that human fetal testis xenografts are resistant to the antiandrogenic effects of a high dose of DBP while also confirming the utility of the model for measuring antiandrogenicity.

Dose Selection

Given the limited number of samples available for this study, DBP dose was carefully considered, and 500 mg/kg/d DBP was chosen as the best dose for comparison with existing studies in the literature. A dose of 500 mg/kg/d DBP reduced accessory sex organ weights in the rat xenograft study by Mitchell *et al.* (2012) and reduced expression of genes involved in testosterone biosynthesis in the rat xenograft study by Heger *et al.* (2012). In the rat *in vivo*, doses of DBP ranging from 100 to 500 mg/kg/d during the late gestational period have been sufficient to reduce testicular testosterone (Carruthers and Foster,

TABLE 3
Significant Genes in Real-time PCR Analysis Compared With Microarray

Gene symbol	Gene ID	Microarray fold change	<i>q</i>	Real-time PCR fold change	<i>p</i>
Vehicle versus unimplanted					
AKR1C3	8644	1.38	.093	1.93	.011
CYP11B1	1584	2.72	.062	13.09	.007
CYP19A1	1588	8.67	.045	39.41	.019
ESR2	2100	0.77	.130	0.55	.043
FDX1	2230	2.53	.044	3.02	.073
KIT	3815	0.50	.052	0.53	.001
POR	5447	1.69	.045	1.67	.212
Abiraterone versus vehicle					
FDX1	2230	1.20	.084	1.40	.024
GNRH2	2797	1.02	.878	1.41	.023
DBP versus vehicle					
FSHR	2492	0.68	.015	0.60	.203

Table 3 lists all genes that were included in the PCR panel and were significantly differentially regulated according to the microarray ($q < 0.05$), PCR array ($p < 0.05$), or both. Fold change and p or q are shown in bold where significant. Treatments: abiraterone—14 d 75 mg/kg/d abiraterone acetate or vehicle (distilled water with Tween-20) po. DBP—14 d 500 mg/kg/d DBP or vehicle (corn oil) po.

Abbreviations: DBP, di-*n*-butyl phthalate; q , q value determined by limma; p , p value determined by paired t test.

2005; Howdeshell *et al.*, 2008; Mahood *et al.*, 2007; Struve *et al.*, 2009) while not resulting in significant fetal mortality (Howdeshell *et al.*, 2008).

The abiraterone acetate dose was selected based on a smaller body of literature. We chose a dose of 75 mg/kg/d, 1.5 times the 50 mg/kg/d dose that reduced serum testosterone, seminal vesicle, and ventral prostate weight in an adult rat study (Duc *et al.*, 2003) and greater on a per weight basis than the 1000 mg/d dose given to human patients in clinical trials (de Bono *et al.*, 2011). This dose proved effective in reducing testosterone in our xenograft model. There was no significant treatment-associated mortality, and no significant effect on host weight (Fig. 3), an important consideration in reproductive toxicology studies. Therefore, we felt this was an informative dose for comparison with DBP and for confirmation that the model is sensitive to compounds that directly reduce testosterone biosynthesis. Importantly, abiraterone acetate can be used as a positive control in future xenograft studies.

Abiraterone Acetate Is Antiandrogenic in Human Fetal Testis

CYP17A1 inhibition by abiraterone has been well characterized (Jarman *et al.*, 1998). In the present study, abiraterone treatment resulted in a dramatic decrease in host serum testosterone and a trend toward increased progesterone (Figs. 2A and B), consistent with CYP17A1 inhibition. However, abiraterone did not significantly affect the intensity or localization of CYP17A1 protein expression (Figs. 1D and E), which might have been expected based on rat data with the CYP17A1 inhibitor prochloraz (Laier *et al.*, 2006). *SULT2A1*, the product of which is responsible for sulfation of pregnenolone (Rainey and Nakamura, 2008), was upregulated in the present study (Fig. 4C). This could possibly be explained by elevated levels

of pregnenolone, the intermediate between cholesterol and progesterone, in the hosts, but this was not measured directly. Abiraterone exposure also resulted in slight upregulation of *GNRH2*, per PCR (Table 3), which could be a response to low intraxenograft testosterone. *Gnrh* and *Gnrhr* appear to have a role in gonad development and early hormone signaling in the rat (Botte *et al.*, 1998).

In addition to antiandrogenic effects, abiraterone appears to have an impact on tissue development and proliferation in the human fetal testis. *TGFB2* and *MET* are downregulated, and Gene Set Enrichment Analysis indicated that transcriptional genes and genes related to cellular morphogenesis were negatively enriched in abiraterone-treated xenografts (Table 2). Perhaps most interesting, abiraterone-treated xenografts were positively enriched for genes involved in epigenetic control of gene expression, including *DICER1* and several DNA methyltransferase genes. This indicates that a CYP17A1 inhibitor could alter epigenetic programming in the testis, including the germ line, which undergoes major reprogramming of DNA methylation during fetal development (Reik *et al.*, 2001). Although abiraterone does not have wide environmental distribution, this may be a human health concern for other CYP17A1 inhibitors such as prochloraz.

Effects of DBP in Human Fetal Testis Xenografts

The mechanisms of action of DBP, unlike abiraterone, are not well characterized and appear to differ by species, as indicated in several recent reviews (Albert and Jégou, 2013; Johnson *et al.*, 2012; Scott *et al.*, 2009). In the rat, fetal DBP exposure reduces testosterone biosynthesis, possibly through inhibition of cholesterol transport and a decrease in the expression of several genes coding for testosterone biosynthesis enzymes (Thompson *et al.*, 2004). In the mouse, no such decrease in testicular testosterone is observed following *in utero* DBP exposure (Gaido

et al., 2007). Albert and Jégou (2013) argue that the preponderance of rat studies clearly demonstrate antiandrogenic effects of phthalates *in utero*, and mouse exposures largely produce a “pro-androgenic” or “norm-androgenic” effect. However, neither species is necessarily predictive of human response. As in previous human fetal testis studies (Heger *et al.*, 2012; Lambrot *et al.*, 2009; Mitchell *et al.*, 2012), DBP had no effect on androgenic processes in the present study (Figs. 2 and 3). DBP-treated grafts did, however, display a nonsignificant trend toward increased MNGs (Fig. 1, $p = .051$). This is an expected effect, as DBP treatment increases germ-cell multinucleation in rat, mouse, and human fetal testis (Gaido *et al.*, 2007). DBP-treated xenograft gene expression data showed enrichment for genes related to cell cycle arrest and the actin filament (Table 2). Arrest of normal germ cells and collapse of intercellular bridges may be involved in MNG formation, and there is existing evidence that DBP affects vimentin localization in Sertoli cells (Kleymenova *et al.*, 2005). Therefore, the impact of DBP on these processes reveals possible mechanistic targets that should be the subject of further study. DBP also decreased FSHR mRNA expression (Table 3), which may further suggest Sertoli cell effects of DBP, as expression of FSHR mRNA increases with Sertoli cell number during the second trimester in normal human fetal testis (O’Shaughnessy *et al.*, 2007).

Implications for Human Health Risk Assessment of Phthalates

Human studies comprise a small proportion of the phthalate literature (Albert and Jégou, 2013), but human fetal testis *in vitro* and xenograft studies have indicated that the human fetal testis differs from the rat in its sensitivity to the antiandrogenic effects of phthalates. DBP has not had significant effects on circulating hormones or organ weights in human fetal testis xenograft studies, despite significant effects in rat xenografts. However, phthalates consistently alter the histology of the seminiferous cord in both *in vitro* and xenograft studies (Heger *et al.*, 2012; Lambrot *et al.*, 2009; Mitchell *et al.*, 2012). The testis is susceptible to formation of MNGs following DBP exposure, without changes in androgen levels (Johnson *et al.*, 2012), and these changes in the seminiferous cord could have ramifications for germline health (Saffarini *et al.*, 2012). Ultimately, in order to assess the human health risk posed by *in utero* exposure to phthalates, additional effort must be made to identify the apparently disparate initiating events leading to the Leydig cell (antiandrogenic) and seminiferous cord effects of phthalates, and to determine the responsiveness of human fetal testis to each of these effects at relevant doses. The TDS hypothesis states that Sertoli and germ cells, in addition to Leydig cells, are potential targets for perturbation of developing testis (Toppari *et al.*, 2010), and so persistent effects on testis could be caused by developmental perturbations of the seminiferous cord as realistically as antiandrogenic effects.

Future studies should employ phthalates other than DBP, as well as mixtures of phthalates, which have additive effects in the rat (Howdeshell *et al.*, 2008).

Utility of the Human Fetal Testis Xenograft Model for Testing Antiandrogens

We have confirmed that a xenograft model can be used to detect an antiandrogenic effect in human fetal testis. Additionally, by including ungrafted control mice, we were able to quantify serum testosterone levels in the castrate host, which should largely derive from the host adrenal gland (Albert and Jégou, 2013). Sham testosterone levels were 20%–25% of those in hosts bearing grafts (Fig. 2), and neither treatment significantly affected sham serum hormone levels, suggesting that adrenal testosterone is unlikely to interfere with assessment of xenograft-derived testosterone. Phthalate metabolism and kinetics are concerns that should be fully addressed in future xenograft studies, although metabolism does not appear to differ greatly among species. DBP is metabolized to the active metabolite monobutyl phthalate (MBP) rapidly, and MBP peaks within 2h following a single dose in pregnant mice (Gaido *et al.*, 2007). Similarly, DBP appears to be metabolized rapidly in humans, primarily to MBP (Koch *et al.*, 2012). Human and mouse metabolism of diethylhexyl phthalate does differ but to a lesser degree than interindividual differences among humans (Ito *et al.*, 2013). Windows of susceptibility to antiandrogenic effects are another concern that should be further characterized in the xenograft model. Although this window has been approximated in previous reports, eg, 8–14 weeks gestation in Scott *et al.* (2009) and 8–12 weeks in Mazaud-Guittot *et al.* (2013), in the current study, gestational week 16–22 testes were clearly still susceptible to disruption by abiraterone acetate.

In characterizing the effects of the xenograft model on gene expression, we found significant differences between unimplanted testis and vehicle-treated xenografts (Figs. 4A and B, Supplementary Table S1). The large number of differentially regulated genes could be driven by several factors, including the effective 4-week age difference between the unimplanted sample and its matched vehicle-treated xenograft sample, hCG stimulation, or other aspects of the renal subcapsular environment of the athymic nude mouse host. The major steroidogenesis-related changes following xenografting were significant increases in expression of *CYP11B1* and *CYP19A1*. Given that the testis xenografts were stimulated with a high dose of hCG, testosterone levels in the xenografts may have induced aromatase expression. Small noncoding RNAs also appear to have a significant role in either the normal maturation of the testis or the adaptation to the xenograft environment (Supplementary Table S1). Small RNAs with altered expression levels included those with known roles in the testis, including *SNORD116* genes (Cassidy *et al.*, 2012) and the *LET7* family of microRNAs (Rakoczy *et al.*, 2013). However, it should be cautioned that microRNAs can be packaged and stably transported in circulating blood (Kosaka *et al.*, 2010) and are highly conserved

across species, meaning that these microRNAs may not have originated in the xenografts. Also, the RNA preparation procedure used for this experiment is presumed to be size selective for RNAs > 200 nt. Therefore, the roles of these microRNAs in the human fetal testis have not been fully characterized. This would require additional experiments aimed at quantifying small RNAs.

CONCLUSIONS

This study confirmed our hypothesis: in hosts bearing human fetal testis xenografts, abiraterone acetate treatment led to a reduction in testosterone, whereas 500 mg/kg/d DBP did not. This result is consistent with several recent findings that human fetal testis is relatively insensitive to direct antiandrogenic actions of DBP but not to the seminiferous cord effects of DBP. We further determined that a Hershberger-like xenograft bioassay can detect antiandrogenic effects in human fetal testis tissue. Humans are exposed to potentially antiandrogenic xenobiotics on a regular basis, including during pregnancy. Based on the available evidence, exposure to antiandrogens *in utero* can dramatically impair the testosterone-dependent development of the male reproductive tract. Numerous industrial, pharmaceutical, and agricultural compounds have antiandrogenic effects in rodents. In addition to studying these compounds in rodents *in utero*, antiandrogenic effects can be assessed in human fetal testis directly using a xenograft system.

SUPPLEMENTARY DATA

Supplementary data are available online at <http://toxsci.oxfordjournals.org/>.

FUNDING

United States Environmental Protection Agency (RD-83459401); National Institute of Environmental Health Sciences at the National Institutes of Health (R01-ES017272, P20, T32-ES7272 to D.J.S.).

ACKNOWLEDGMENTS

The authors are deeply grateful to the parents who consented to participate in this study. They thank Kristen Delayo for coordinating tissue donations, Christoph Schorl for microarray processing, and Melinda Golde and Paula Weston for processing histological samples. They also thank the University of Virginia Center for Research in Reproduction for serum hormone analyses. The University of Virginia Center for Research in Reproduction Ligand Assay and Analysis Core is supported by the Eunice Kennedy Shriver NICHD/NIH (SCCPIR) Grant U54-HD28934. K. B. does occasional expert consulting with

pharmaceutical companies (Akros, Pfizer, Global Alliance for Tb Drug Development, Zafgen). He also owns stock in Exxon-Mobil and Pfizer and in a small start-up biotechnology company (CytoSolv) developing a wound-healing therapeutic.

REFERENCES

- Albert, O., and Jégou, B. (2013). A critical assessment of the endocrine susceptibility of the human testis to phthalates from fetal life to adulthood. *Hum Reprod Update*. doi:10.1093/humupd/dmt1050.
- Andersen, C. L., Jensen, J. L., and Orntoft, T. F. (2004). Normalization of real-time quantitative reverse transcription-PCR data: A model-based variance estimation approach to identify genes suited for normalization, applied to bladder and colon cancer data sets. *Cancer Res*. **64**, 5245–5250.
- Botte, M. C., Chamagne, A. M., Carre, M. C., Counis, R., and Kottler, M. L. (1998). Fetal expression of GnRH and GnRH receptor genes in rat testis and ovary. *J. Endocrinol*. **159**, 179–189.
- Brazma, A., Hingamp, P., Quackenbush, J., Sherlock, G., Spellman, P., Stoeckert, C., Aach, J., Ansorge, W., Ball, C. A., Causton, H. C. *et al.* (2001). Minimum information about a microarray experiment (MIAME)-toward standards for microarray data. *Nat. Genet*. **29**, 365–371.
- Carruthers, C. M., and Foster, P. M. (2005). Critical window of male reproductive tract development in rats following gestational exposure to di-n-butyl phthalate. *Birth Defects Res. B Dev. Reprod. Toxicol*. **74**, 277–285.
- Carvalho, B. S., and Irizarry, R. A. (2010). A framework for oligonucleotide microarray preprocessing. *Bioinformatics* **26**, 2363–2367.
- Cassidy, S. B., Schwartz, S., Miller, J. L., and Driscoll, D. J. (2012). Prader-Willi syndrome. *Genet Med*. **14**, 10–26.
- de Bono, J. S., Logothetis, C. J., Molina, A., Fizazi, K., North, S., Chu, L., Chi, K. N., Jones, R. J., Goodman, O. B., Jr, Saad, F., *et al.* (2011). Abiraterone and increased survival in metastatic prostate cancer. *N. Engl. J. Med*. **364**, 1995–2005.
- De Paepe, M. E., Chu, S., Heger, N., Hall, S., and Mao, Q. (2012). Resilience of the human fetal lung following stillbirth: Potential relevance for pulmonary regenerative medicine. *Exp. Lung Res*. **38**, 43–54.
- Duc, I., Bonnet, P., Duranti, V., Cardinali, S., Riviere, A., De Giovanni, A., Shields-Botella, J., Barcelo, G., Adje, N., Carniato, D., *et al.* (2003). In vitro and in vivo models for the evaluation of potent inhibitors of male rat 17alpha-hydroxylase/C17,20-lyase. *J. Steroid Biochem. Mol. Biol*. **84**, 537–542.
- Gaido, K. W., Hensley, J. B., Liu, D., Wallace, D. G., Borghoff, S., Johnson, K. J., Hall, S. J., and Boekelheide, K. (2007). Fetal mouse phthalate exposure shows that gonocyte multinucleation is not associated with decreased testicular testosterone. *Toxicol. Sci*. **97**, 491–503.
- Gray, L. E., Jr., Furr, J., and Ostby, J. S. (2005). Hershberger assay to investigate the effects of endocrine-disrupting compounds with androgenic or antiandrogenic activity in castrate-immature male rats. *Curr. Protoc. Toxicol*. **26**, 16.9.1–16.9.15.
- Haidar, S., Ehmer, P. B., Barassin, S., Batzl-Hartmann, C., and Hartmann, R. W. (2003). Effects of novel 17alpha-hydroxylase/C17, 20-lyase (P450 17, CYP 17) inhibitors on androgen biosynthesis in vitro and in vivo. *J. Steroid Biochem. Mol. Biol*. **84**, 555–562.
- Heger, N. E., Hall, S. J., Sandrof, M. A., McDonnell, E. V., Hensley, J. B., McDowell, E. N., Martin, K. A., Gaido, K. W., Johnson, K. J., and Boekelheide, K. (2012). Human fetal testis xenografts are resistant to phthalate-induced endocrine disruption. *Environ. Health Perspect*. **120**, 1137–1143.
- Howdeshell, K. L., Wilson, V. S., Furr, J., Lambright, C. R., Rider, C. V., Blystone, C. R., Hotchkiss, A. K., and Gray, L. E., Jr. (2008). A mixture of five phthalate esters inhibits fetal testicular testosterone production in the sprague-dawley rat in a cumulative, dose-additive manner. *Toxicol. Sci*. **105**, 153–165.

- Ito, Y., Kamijima, M., Hasegawa, C., Tagawa, M., Kawai, T., Miyake, M., Hayashi, Y., Naito, H., and Nakajima, T. (2013). Species and inter-individual differences in metabolic capacity of di(2-ethylhexyl)phthalate (DEHP) between human and mouse livers. *Environ. Health Prev. Med.* doi:10.1007/s12199-12013-10362-12196.
- Jarman, M., Barrie, S. E., and Llera, J. M. (1998). The 16,17-double bond is needed for irreversible inhibition of human cytochrome p45017alpha by abiraterone (17-(3-pyridyl)androsta-5, 16-dien-3beta-ol) and related steroidal inhibitors. *J. Med. Chem.* **41**, 5375–5381.
- Johnson, K. J., Heger, N. E., and Boekelheide, K. (2012). Of mice and men (and rats): Phthalate-induced fetal testis endocrine disruption is species-dependent. *Toxicol. Sci.* **129**, 235–248.
- Klymenova, E., Swanson, C., Boekelheide, K., and Gaido, K. W. (2005). Exposure in utero to di(n-butyl) phthalate alters the vimentin cytoskeleton of fetal rat Sertoli cells and disrupts Sertoli cell-gonocyte contact. *Biol. Reprod.* **73**, 482–490.
- Koch, H. M., Christensen, K. L., Harth, V., Lorber, M., and Bruning, T. (2012). Di-n-butyl phthalate (DnBP) and diisobutyl phthalate (DiBP) metabolism in a human volunteer after single oral doses. *Arch. Toxicol.* **86**, 1829–1839.
- Kosaka, N., Iguchi, H., Yoshioka, Y., Takeshita, F., Matsuki, Y., and Ochiya, T. (2010). Secretory mechanisms and intercellular transfer of microRNAs in living cells. *J. Biol. Chem.* **285**, 17442–17452.
- Laier, P., Metzдорff, S. B., Borch, J., Hagen, M. L., Hass, U., Christiansen, S., Axelstad, M., Kledal, T., Dalgaard, M., McKinnell, C., et al. (2006). Mechanisms of action underlying the antiandrogenic effects of the fungicide prochloraz. *Toxicol. Appl. Pharmacol.* **213**, 160–171.
- Lambrot, R., Muczynski, V., Lecureuil, C., Angenard, G., Coffigny, H., Pairault, C., Moison, D., Frydman, R., Habert, R., and Rouiller-Fabre, V. (2009). Phthalates impair germ cell development in the human fetal testis in vitro without change in testosterone production. *Environ. Health Perspect.* **117**, 32–37.
- Leek, J. T., Johnson, W. E., Parker, H. S., Jaffe, A. E., and Storey, J. D. (2012). The sva package for removing batch effects and other unwanted variation in high-throughput experiments. *Bioinformatics* **28**, 882–883.
- Li, A. (2013). hugene10stranscriptcluster.db: Affymetrix Human Gene 1.0-ST Array Transcriptcluster Revision 8 annotation data (chip hugene10stranscriptcluster), R package version 8.0.1. Available at: <http://www.bioconductor.org/packages/release/data/annotation/html/hugene10stranscriptcluster.db.html>.
- Livak, K. J., and Schmittgen, T. D. (2001). Analysis of relative gene expression data using real-time quantitative PCR and the 2(-Delta Delta C(T)) Method. *Methods* **25**, 402–408.
- Lottrup, G., Andersson, A. M., Leffers, H., Mortensen, G. K., Toppari, J., Skakkebaek, N. E., and Main, K. M. (2006). Possible impact of phthalates on infant reproductive health. *Int. J. Androl.* **29**, 172–180.
- Mahood, I. K., Scott, H. M., Brown, R., Hallmark, N., Walker, M., and Sharpe, R. M. (2007). In utero exposure to di(n-butyl) phthalate and testicular dysgenesis: Comparison of fetal and adult end points and their dose sensitivity. *Environ. Health Perspect.* **115**(Suppl. 1), 55–61.
- Mazaud-Guittot, S., Nicolaz, C. N., Desdoits-Lethimonier, C., Coiffec, I., Maamar, M. B., Balaguer, P., Kristensen, D. M., Chevrier, C., Lavoue, V., Poulain, P., et al. (2013). Paracetamol, aspirin and indomethacin induce endocrine disturbances in the human fetal testis capable of interfering with testicular descent. *J. Clin. Endocrinol. Metab.* doi:10.1210/jc.2013-2531.
- Miller, W. L. and R. J. Auchus (2011). The molecular biology, biochemistry, and physiology of human steroidogenesis and its disorders. *Endocr Rev* **32**, 81–151.
- Mitchell, R. T., Childs, A. J., Anderson, R. A., van den Driesche, S., Saunders, P. T., McKinnell, C., Wallace, W. H., Kelnar, C. J., and Sharpe, R. M. (2012). Do phthalates affect steroidogenesis by the human fetal testis? Exposure of human fetal testis xenografts to di-n-butyl phthalate. *J. Clin. Endocrinol. Metab.* **97**, E341–E348.
- Moffit, J. S., Her, L. S., Mineo, A. M., Knight, B. L., Phillips, J. A., and M. S. Thibodeau (2013). Assessment of inhibin B as a biomarker of testicular injury following administration of carbendazim, cetrorelix, or 1,2-dibromo-3-chloropropane in wistar han rats. *Birth Defects Res. B Dev. Reprod. Toxicol.* **98**, 17–28.
- O'Shaughnessy, P. J., Baker, P. J., Monteiro, A., Cassie, S., Bhattacharya, S., and Fowler, P. A. (2007). Developmental changes in human fetal testicular cell numbers and messenger ribonucleic acid levels during the second trimester. *J. Clin. Endocrinol. Metab.* **92**, 4792–4801.
- Pfaffl, M. W., Tichopad, A., Prgomet, C., and Neuvians, T. P. (2004). Determination of stable housekeeping genes, differentially regulated target genes and sample integrity: BestKeeper—Excel-based tool using pair-wise correlations. *Biotechnol. Lett.* **26**, 509–515.
- R Core Team (2012). *R: A Language and Environment for Statistical Computing*. R Foundation for Statistical Computing, Vienna, Austria.
- Rainey, W. E., and Nakamura, Y. (2008). Regulation of the adrenal androgen biosynthesis. *J. Steroid Biochem. Mol. Biol.* **108**, 281–286.
- Rakoczy, J., Fernandez-Valverde, S. L., Glazov, E. A., Wainwright, E. N., Sato, T., Takada, S., Combes, A. N., Korbie, D. J., Miller, D. J., Grimmond, S. M., et al. (2013). MicroRNAs-140-5p/140-3p modulate Leydig cell numbers in the developing mouse testis. *Biol. Reprod.* **88**, 143.
- Reich, M., Liefeld, T., Gould, J., Lerner, J., Tamayo, P., and Mesirov, J. P. (2006). GenePattern 2.0. *Nat. Genet.* **38**, 500–501.
- Reik, W., Dean, W., and Walter, J. (2001). Epigenetic reprogramming in mammalian development. *Science* **293**, 1089–1093.
- Rider, C. V., Furr, J., Wilson, V. S., and Gray, L. E., Jr. (2008). A mixture of seven antiandrogens induces reproductive malformations in rats. *Int. J. Androl.* **31**, 249–262.
- Saffarini, C. M., Heger, N. E., Yamasaki, H., Liu, T., Hall, S. J., and Boekelheide, K. (2012). Induction and persistence of abnormal testicular germ cells following gestational exposure to di-(n-butyl) phthalate in p53-null mice. *J. Androl.* **33**, 505–513.
- Scott, H. M., Mason, J. I., and Sharpe, R. M. (2009). Steroidogenesis in the fetal testis and its susceptibility to disruption by exogenous compounds. *Endocr. Rev.* **30**, 883–925.
- Smyth, G. (2005). Limma: Linear models for microarray data. In *Bioinformatics and Computational Biology Solutions Using R and Bioconductor* (R. Gentleman, V. Carey, S. Dudoit, R. A. Irizarry, and W. Huber, Eds.), pp. 397–420 Springer, New York.
- Struve, M. F., Gaido, K. W., Hensley, J. B., Lehmann, K. P., Ross, S. M., Sochaski, M. A., Willson, G. A., and Dorman, D. C. (2009). Reproductive toxicity and pharmacokinetics of di-n-butyl phthalate (DBP) following dietary exposure of pregnant rats. *Birth Defects Res. B Dev. Reprod. Toxicol.* **86**, 345–354.
- Subramanian, A., Tamayo, P., Mootha, V. K., Mukherjee, S., Ebert, B. L., Gillette, M. A., Paulovich, A., Pomeroy, S. L., Golub, T. R., Lander, E. S., et al. (2005). Gene set enrichment analysis: A knowledge-based approach for interpreting genome-wide expression profiles. *Proc. Natl. Acad. Sci. U.S.A.* **102**, 15545–15550.
- Thompson, C. J., Ross, S. M., and Gaido, K. W. (2004). Di(n-butyl) phthalate impairs cholesterol transport and steroidogenesis in the fetal rat testis through a rapid and reversible mechanism. *Endocrinology* **145**, 1227–1237.
- Toppari, J., Virtanen, H. E., Main, K. M., and Skakkebaek, N. E. (2010). Cryptorchidism and hypospadias as a sign of testicular dysgenesis syndrome (TDS): Environmental connection. *Birth Defects Res. A Clin. Mol. Teratol.* **88**, 910–919.
- Unni, S. K., Modi, D. N., Pathak, S. G., Dhabalia, J. V., and Bhartiya, D. (2009). Stage-specific localization and expression of c-kit in the adult human testis. *J. Histochem. Cytochem.* **57**, 861–869.